

# On data and dimension in chemistry I - irreversibility, concealment and emergent conservation laws

Alex Blokhuis<sup>Ⓛ\*</sup>

*Stratingh Institute for Chemistry, University of Groningen,  
Nijenborgh 4, 9747 AG Groningen, the Netherlands  
Groningen Institute for Evolutionary Life Sciences, University of Groningen,  
Nijenborgh 4, 9747 AG Groningen, the Netherlands  
University of Strasbourg & CNRS, UMR7140, 67083 Strasbourg, France and  
Instituto IMDEA Nanociencia, Calle Faraday 9, 28049 Madrid, Spain*

Martijn van Kuppeveld<sup>Ⓛ</sup>

*Stratingh Institute for Chemistry, University of Groningen,  
Nijenborgh 4, 9747 AG Groningen, the Netherlands*

Daan van de Weem

*Scuola Internazionale Superiore di Studi Avanzati (SISSA), Via Bonema 265, 34136 Trieste, Italy*

Robert Pollice<sup>Ⓛ†</sup>

*Stratingh Institute for Chemistry, University of Groningen,  
Nijenborgh 4, 9747 AG Groningen, the Netherlands*

(Dated: April 9, 2024)

Chemical systems are interpreted through the species they contain and the reactions they may undergo, i.e., their chemical reaction network (CRN). In spite of their central importance to chemistry, the structure of CRNs continues to be challenging to deduce from data. Although there exist structural laws relating species, reactions, conserved quantities and cycles, there has been limited attention to their measurable consequences. One such is the *dimension* of the chemical data: the number of independent reactions, i.e. the number of measured variables minus the number of constraints. In this paper we attempt to relate the experimentally observed dimension to the structure of the CRN.

In particular, we investigate the effects of species that are concealed and reactions that are irreversible. For instance, irreversible reactions can have proportional rates. The resulting reduction in degrees of freedom can be captured by the *co-production law*  $\Upsilon = \mathfrak{a}_{\bullet} + \mathfrak{A}_{\bullet}$ , relating co-production relations  $\Upsilon$  to emergent non-integer conservation laws  $\mathfrak{a}_{\bullet}$  and broken cycles  $\mathfrak{A}_{\bullet}$ . This law resolves a recent conundrum posed by a machine-discovered candidate for a non-integer conservation law. We also obtain laws that allow us to relate data dimension to network structure in cases where some species cannot be discerned or distinguished by a given analytical technique, allowing to better narrow down what CRNs can underly experimental data.

## I. INTRODUCTION

Our capacity to build [1–10] and understand [11–26] chemical systems of increasing complexity is intimately tied to our understanding of their reaction networks and our ability to elucidate them. Whereas sizeable molecular structures can be elucidated today, reconstructing the structure of even small reaction networks remains challenging [27]. Our understanding of theoretical CRN dynamics does not yet fully address the practical matter of relating their structure to experimental observation.

From a data perspective, prospects are ever brighter: There have been leaps in standardiza-

tion and reproducibility due to increased automation in e.g. synthesis [28–31] and reaction monitoring [32–36], which has enabled the collection of comparably large high quality datasets. Simultaneously, new methods continue to be developed to resolve what was previously invisible or indistinguishable. A few such methods are delayed reactant labeling [37, 38], nonlinear effects for enantiomers and excess [39–41], its extension to derivatives and rates [42], time-dependent illumination protocols [43], oscillating temperature [44] or concentration protocols. As chemical data becomes more precise and captures additional details, deeper signatures of the underlying systems are revealed [45].

The ever increasing availability of larger datasets characterizing CRNs in turn increases the utility of automating analysis steps. The interpretability of chemical data - for instance from spectroscopy - can be improved dramati-

\* alex\_blokhuis@hotmail.com

† r.pollice@rug.nl

ically through multivariate curve resolution (MCR) techniques that seek to decompose a series of spectra of a mixture into a factorization of spectra of pure components and their concentrations[46–53]. An intrinsic obstacle for MCR approaches - known as rotational ambiguity - is that this factorization is not unique.

Usually, chemical data does not capture all species present in any given system, and many CRN hypotheses could be proposed to explain said data. Naturally, one can directly compare the measurement data to the output of a candidate CRN. However, limited conclusions can be drawn from this fit alone[54–56], as one can not exhaust all other possible CRNs this way. Recent approaches include alternative means of assessing more CRNs or assessing them more rigorously, e.g., through mechanism test functions[44], Bayesian ERN analysis[57], first-passage time distributions [58, 59], and increasingly generalized assessments of reaction orders[60–63]. However, exhaustive CRN assessment is as of yet not within reach.

In 1963, R. Aris reported on the experimental possibility of establishing the number of independent reactions from concentration-time data in a stirred tank reactor[64] through linear algebra. Motivated by such insight and examples set by other fields, CRN theory started to develop shortly after[11]. One important pillar of CRN theory is the establishment of structural criteria[13, 22, 65–67] for the onset or absence of complex behavior (e.g., oscillations, multistability, chaos). Another pillar is nonequilibrium thermodynamics[11, 12, 68, 69] applied to chemistry in a wealth of contexts, [12, 70–73], including its connections to complex behavior[69, 74, 75]. In their study, CRNs have been principally approached from a perspective where they are known *a priori*. As the CRN deduction problem remains open, it seems fitting to reinvestigate the 1963 viewpoint of an observer interpreting chemical data from an unknown CRN.

In this paper, we consider the *dimensional indices* of chemical data a CRN would produce and how it manifests in a series of spectroscopic measurements. The first dimension we discuss is the number of discernible independent reactions,  $d = \#$  measured variables  $-\#$  constraints. First, we derive what we call the *co-production law*, which captures emergent non-integer conservation laws and broken cycles due to collinear reactions, and demonstrate that it resolves a conundrum posed by an anomalous conservation law recently discovered[76]. Subsequently, we derive one dimension law for concealed species

and another one for indistinguishable species. Finally, we describe how determining these dimensions from the experimental data relates portions of data to specific parts of the CRN structure. An overview of important quantities can be found in the glossary in Appendix A.

## II. EXCESS CONSERVATION: AN EXAMPLE

Our overarching aim is to relate conservation laws to CRN structure. Currently, theories do not capture all such laws yet. We will thus dedicate the next few sections to extending the theory of conservation laws in CRNs, using as a motivating example a system with one conservation law in excess of those predicted.

As an insightful example in which a new conservation law emerges, we will consider the CRNs in Fig. 1. We consider  $s = 4$  species, and  $r = 2$  bimolecular reactions



For mass-action kinetics, we obtain ordinary differential equations (ODEs)

$$\begin{aligned} d_t[A] &= -(\kappa_1 + \kappa_2)[A][B] + \kappa_3[C] + \kappa_4[D], \\ d_t[B] &= -(\kappa_1 + \kappa_2)[A][B] + \kappa_3[C] + \kappa_4[D], \\ d_t[C] &= \kappa_1[A][B] - \kappa_3[C], \\ d_t[D] &= \kappa_2[A][B] - \kappa_4[C]. \end{aligned}$$

We can predict the number of linear conservation laws, which are laws of the form

$$L = \sum_k \ell_k [X_k]. \quad (2)$$

Assuming conservation laws are due to stoichiometry only, we would predict to have exactly  $\ell = s - r = 2$  linear conservation laws,

$$\begin{aligned} L^{(1)} &= [A] + [C] + [D], \\ L^{(2)} &= [B] + [C] + [D]. \end{aligned}$$

which is correct.

However, when both reactions are rendered irreversible, that is



an additional conserved quantity appears. Since now  $\kappa_3 = \kappa_4 = 0$ , it follows from inspection that

$$d_t[C] = \frac{\kappa_1}{\kappa_2} d_t[D] = \kappa_1[A][B]. \quad (4)$$

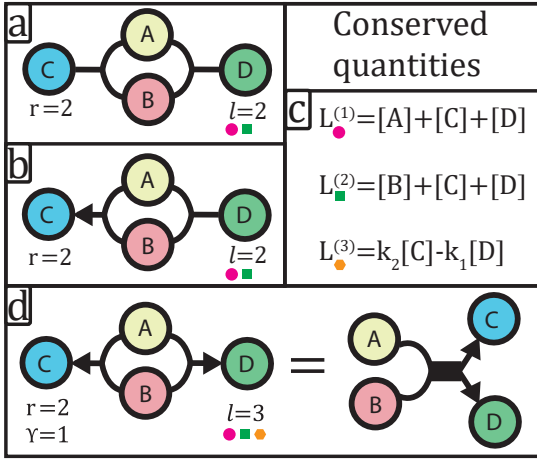


FIG. 1: a-b) CRNs whose conservation laws follow from integer stoichiometry. c) conservation laws. Making reactions  $r_1, r_2$  irreversible, an additional non-integer conservation conserved quantity  $L^{(3)}$  emerges. d) CRN with an emergent non-integer conserved quantity. For integer stoichiometry, such quantities do not follow from the first structural law (Eq.15).  $r$  : # reactions,  $\ell$  : # conserved quantities,  $\Upsilon$ : co-production index, # collinear reactions. Species are represented by nodes. Reactants (resp. products) in a reaction are joined by round arcs.

Thus  $\ell = 3$ , i.e., a novel type of conservation law with non-integer coefficients emerged

$$L^{(3)} = k_2[C] - k_1[D], \quad (5)$$

which does not follow from stoichiometry. As a shorthand, such emergent invariants will be referred to as *emanants*.

Importantly, if we monitored both the reversible CRN (1) and the irreversible CRN (3) spectroscopically (Fig. 2), we would - provided spectral overlap - observe an isosbestic[77–80] point for CRN (3), but not for CRN (1). This is an immediate observable consequence of an additional conservation law lowering the dimension.[81]

Thus, conserved quantities need not derive from (classical) stoichiometry alone. This forms the motivation to reinspect how conservation laws in CRNs are derived, and extend this formalism to count chemically meaningful quantities that are missed via standard approaches.

### III. STOICHIOMETRIC MATRICES

We will now reinspect CRN theory from the point of view of stoichiometry, and subsequently

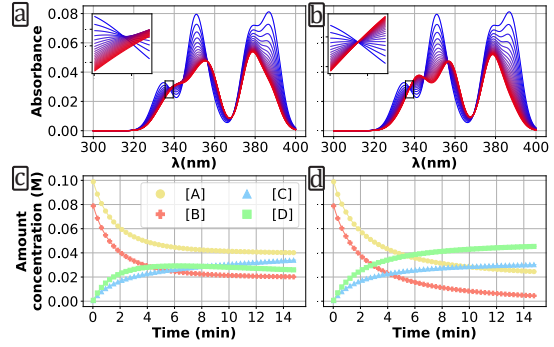
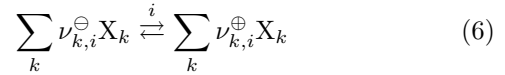
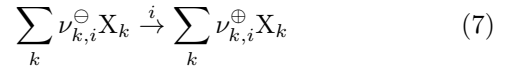


FIG. 2: (a) Simulated absorption spectra for CRN  $C \rightleftharpoons A + B \rightleftharpoons D$ , no isosbestic point ( $d(\Lambda) = 2$ ). b) simulated spectra for CRN  $C \leftarrow A + B \rightarrow D$ , a close-up reveals an isosbestic point ( $d(\Lambda) = 1$ ). (c) Underlying dynamics for a)  $\kappa = (2.0, 0.03, 3.0, 0.11)$ , d) underlying dynamics for b).  $\kappa = (2.0, 0, 3.0, 0)$ . For both,  $[X]_0 = (0.1, 0.08, 0, 0)$

identify where this analysis can overlook conservation laws. A reversible chemical reaction  $r_i^\circ$  is represented as



where  $\nu_{k,i}^\ominus, \nu_{k,i}^\oplus$  are integer stoichiometric coefficients. Similarly, an irreversible reaction  $r_i^\triangleright$  is represented as

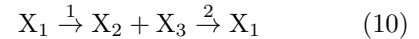
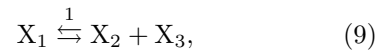


We can then define a stoichiometric matrix by taking the difference in the indices

$$\mathbb{S} = \nu^\oplus - \nu^\ominus, \quad (8)$$

and we refer to  $\nu^\ominus$  (resp.  $\nu^\oplus$ ) as the stoichiometric reactant (resp. product) matrix. We endow  $\mathbb{S}$  with a suffix  $\mathbb{S}_\circ$  (resp.  $\mathbb{S}_\triangleright$ ) to refer to descriptions in terms of reversible (resp. irreversible) reactions.

Formally, a reversible reaction can be built up from a pair of opposing irreversible reactions,

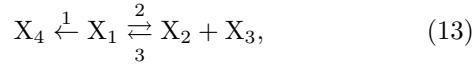


$$\mathbb{S}_\circ = \begin{pmatrix} -1 \\ 1 \\ 1 \end{pmatrix}, \quad \mathbb{S}_{\triangleright} = \begin{pmatrix} -1 & 1 \\ 1 & -1 \\ 1 & -1 \end{pmatrix}. \quad (11)$$

For a fully reversible chemical reaction network (CRN), we can always represent the same CRN in terms of pairs of irreversible reaction steps

$$\mathbb{S}_{\triangleright, \text{reversible CRN}} = (\mathbb{S}_\circ, -\mathbb{S}_\circ) \quad (12)$$

Conversely, if at least some reactions do not have a reverse, we can only fully represent the CRN using  $\mathbb{S}_{\triangleright}$ , for instance



$$\mathbb{S}_{\triangleright} = \begin{pmatrix} -1 & -1 & 1 \\ 0 & 1 & -1 \\ 0 & 1 & -1 \\ 1 & 0 & 0 \end{pmatrix}. \quad (14)$$

Thermodynamically, reactions have a microscopic reverse. Irreversible reactions can parsimoniously describe kinetics when this reverse becomes negligible enough[82]. This can for instance occur when products disappear from the reaction medium (e.g. as gas or precipitate), or for reactions with high driving forces. The latter is of special importance for the production and subsequent reaction of highly reactive species, as occurs in radiochemistry, plasma chemistry and photochemistry. Irreversible reactions are thus of chemistry-wide importance, but particularly prevalent in some branches of chemistry such as astrochemistry[83–85], photochemical motors[86, 87] and atmospheric chemistry[88–90].

### A. The first structural law (SL1)

Dimensions of fundamental subspaces of  $\mathbb{S}$  count quantities with a chemical interpretation, through the fundamental theorem of linear algebra (FTLA). We refer to the following relation [11, 12] as the first structural law (SL1):

$$\text{rk}(\mathbb{S}) = s - \ell = r - c \quad (15)$$

Letting  $\#$  denote 'the number of', we have:

- rk( $\mathbb{S}$ ): rank of matrix  $\mathbb{S}$
- $s$ : # species ( $X_1, \dots, X_s$ )
- $\ell$ : # conserved quantities ( $\dim(\text{coker}(\mathbb{S}))$ )
- $r$ : # reactions ( $r_1, \dots, r_r$ )
- $c$ : # cycles ( $\dim(\text{ker}(\mathbb{S}))$ )

The number of conserved quantities (resp. cycles) are thus directly related to the dimension of the left (resp. right) nullspace, i.e. of the cokernel (resp. kernel) of  $\mathbb{S}$ . The fundamental theorem of linear algebra (FTLA) provides two ways to count the rank in terms of chemical quantities, thus giving us a combinatorial identity (SL1) (Eq. (15)) that relates them. SL1 thereby relates fundamental CRN quantities based on structure.

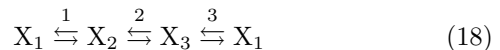
### B. Stoichiometric interpretation of SL1

We will now take a closer look at the number of cycles ( $c$ ) and conserved quantities ( $\ell$ ). These correspond respectively to  $c$  right nullvectors and  $\ell$  left nullvectors

$$\mathbb{S} \mathbf{c}^{(i)} = \mathbf{0}, \quad (i \in \{0, \dots, c\}) \quad (16)$$

$$\boldsymbol{\ell}^{(i)} \mathbb{S} = \mathbf{0} \quad (i \in \{0, \dots, \ell\}) \quad (17)$$

Usually, cycles are interpreted as combinations of reactions that leave the system unchanged and the constraints are interpreted as integer combinations of species that remain unchanged. For instance, the network below (Fig. 3) has  $s = r = 3, \ell = c = 1$



$$\mathbb{S}_o = \begin{pmatrix} -1 & 0 & 1 \\ 1 & -1 & 0 \\ 0 & 1 & -1 \end{pmatrix} \quad (19)$$

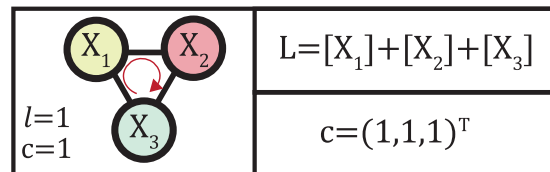


FIG. 3: A small cyclic CRN.  $\ell$ : # conserved quantities.  $c$ : # cycles.

Performing reactions 1, 2, and 3 in equal amounts leaves the system unchanged

$$\begin{pmatrix} \Delta[X_1] \\ \Delta[X_2] \\ \Delta[X_3] \end{pmatrix} = \mathbb{S} \begin{pmatrix} 1 \\ 1 \\ 1 \end{pmatrix} = \mathbf{0} \quad (20)$$

and the following integer combination of species is conserved

$$L = [X_1] + [X_2] + [X_3]. \quad (21)$$

Notably, stoichiometric constraints are known by many names[91], for instance, conserved charges[67], components, invariants[11], conserved quantities[12], or conservation laws[76].

We will see later that the application to dynamics requires an extension of the above interpretation of cycles and conservation laws. In anticipation of this extension - in which cycles may vanish and additional conservation laws emerge - we will henceforth add a suffix to the conserved quantities and cycles we counted without this extension, and count their number as  $\ell_o, c_o$ .

For the stoichiometric matrix  $\mathbb{S}_{\triangleright}$  all reactions are encoded as one-way reactions. We

denote the number of reactions that have a reverse by  $r_{\bowtie}$ . Performing a pair of conjugate reactions leaves the system unchanged, yielding a trivial 2-membered cycle which we ordinarily do not seek to count. In general we can write

$$\mathbb{S}_o = (\mathbb{S}_{\triangleright}, \mathbb{S}_{\triangleleft}), \quad (22)$$

$$\mathbb{S}_{\bowtie} = (\mathbb{S}_o, -\mathbb{S}_{\triangleleft}) = (\mathbb{S}_{\triangleright}, \mathbb{S}_{\triangleleft}, -\mathbb{S}_{\triangleleft}), \quad (23)$$

where  $\mathbb{S}_{\triangleleft}$  contains the reactions from  $\mathbb{S}_o$  that are reversible. All reactions in  $\mathbb{S}_{\bowtie}$  in excess of those in  $\mathbb{S}_o$  yield 2-cycles, we thus always have  $\text{rk}(\mathbb{S}_{\bowtie}) = \text{rk}(\mathbb{S}_o)$ .

We will now split the established counting of reactions  $r$  and cycles  $c_o$  into their reversible and irreversible components

$$\text{rk}(\mathbb{S}_{\triangleright}) = s - \ell_o = r_{\triangleright} - c_{\triangleright} = r_o - c_o \quad (24)$$

$$c_o = c_{\triangleright} - r_{\triangleleft}. \quad (25)$$

Conventionally,  $r, c$  are used to denote nontrivial reactions and cycles

$$r = r_o, \quad c = c_o. \quad (26)$$

The necessity of further decomposing constraints and cycles emerges from kinetics, which we will introduce next. Conventionally, we have that

### C. Time evolution

The time evolution of species concentrations  $[X_1], \dots, [X_s]$  follows the kinetic equations

$$d_t[\mathbf{X}] = \mathbb{S} \mathbf{J}, \quad (27)$$

where  $\mathbf{J} = (J_1, \dots, J_r)^T$  is a vector of  $r$  reaction currents. We will consider these currents to follow mass-action kinetics[92], so that their expression follows from stoichiometry as

$$J_{i,\triangleright} = \kappa_i \prod_{k=1}^s \nu_{k,i}^{\ominus} [X_k]^{\nu_{k,i}^{\ominus}}. \quad (28)$$

We are ultimately interested in finding linear conservation laws  $L^{(i)}$  with coefficients  $\ell^{(i)}$ .

$$\ell_1^{(i)} [X_1] + \dots + \ell_s^{(i)} [X_s] = L^{(i)}, \quad (29)$$

$$d_t L^{(i)} = 0. \quad (30)$$

Rewriting this equation using the above notation yields

$$d_t \ell^T [\mathbf{X}] = \ell^T \mathbb{S} \mathbf{J} = 0, \quad (31)$$

This formulation shows that the left nullvectors of  $\mathbb{S}$  form a solution, as for these:

$$\ell^T \mathbb{S} = \mathbf{0}. \quad (32)$$

However, these are not necessarily the only solutions. We are ultimately interested in the constant solutions  $\ell^T$  of Eq. (31), where we would like to remark that  $\mathbf{J}$  depends on the concentrations  $[X_k]$ . These solutions then give us the coefficients of the conserved quantities. To see that Eq. (31) can have further solutions, we will now revisit our initial examples of reversible CRN Eq. (1) and irreversible CRN Eq. (3). We then derive a network law for the additional chemical quantities SL1 needs to count when applied to the time evolution of species. Sec.B of the Appendix applies this law to verify and explain the recent algorithmic detection of a non-integer conservation law[76] that was not anticipated, due to not being a solution to Eq. (32).

### D. Hidden irreversible conservation law

We can now address the emergence of further conservation laws by irreversibility. We return to our example



Using mass-action, we have  $r_o = 2$  linearly independent currents

$$J_{1,o} = \kappa_1 [A][B] - \kappa_3 [C] = J_{1,\triangleright} - J_{3,\triangleright}$$

$$J_{2,o} = \kappa_2 [A][B] - \kappa_4 [D] = J_{2,\triangleright} - J_{4,\triangleright}$$

and stoichiometric matrices  $\mathbb{S}_o, \mathbb{S}_{\triangleright}^o$

$$\mathbb{S}_o = \begin{pmatrix} -1 & -1 \\ -1 & -1 \\ 1 & 0 \\ 0 & 1 \end{pmatrix}, \quad \mathbb{S}_{\triangleright}^o = \begin{pmatrix} -1 & -1 & 1 & 1 \\ -1 & -1 & 1 & 1 \\ 1 & 0 & -1 & 0 \\ 0 & 1 & 0 & -1 \end{pmatrix} \quad (34)$$

i.e.  $\mathbb{S}_{\triangleleft} = \mathbb{S}_o$ , so that

$$d_t [\mathbf{X}] = \mathbb{S}_o \mathbf{J}_o = \mathbb{S}_{\triangleright}^o \mathbf{J}_{\triangleright}. \quad (35)$$

i.e., we can represent the same species dynamics using a distinct number of reactions  $r$ . Since we have  $r_o = 2$  linearly independent reactions, we need at least  $r = 2$ .

We now modify the above network by rendering both bimolecular reactions irreversible

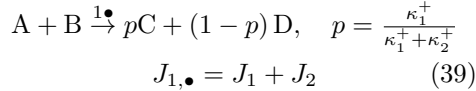


so that  $r_{\gg} = 0$ , and  $\mathbb{S}_{\gg}$  loses its last two columns compared to  $\mathbb{S}_{\gg}^{\circ}$ . We afford the irreversible currents by removing the reverse reaction from  $J_1, J_2$

$$J_{1,\gg} = \kappa_1[A][B], \quad (37)$$

$$J_{2,\gg} = \kappa_2[A][B] = \frac{\kappa_2}{\kappa_1} J_{1,\gg} \quad (38)$$

Dynamically, the reactions are not independent, since the currents are collinear (cf. Eq. (38)). Thus, we only need 1 current and 1 reaction for a deterministic description[93] Hence, we can merge the collinear reactions



We now construct a new stoichiometric matrix  $\mathbb{S}_{\bullet}$  that admits merged reactions

$$\mathbb{S}_{\gg} = \begin{pmatrix} -1 & -1 \\ -1 & -1 \\ 1 & 0 \\ 0 & 1 \end{pmatrix}, \quad \mathbb{S}_{\bullet} = \begin{pmatrix} -1 \\ -1 \\ p \\ 1-p \end{pmatrix}. \quad (40)$$

The time evolution of the system is then fully described by

$$d_t[\mathbf{X}] = \mathbb{S}_{\gg} \mathbf{J}_{\gg} = \mathbb{S}_{\bullet} \mathbf{J}_{\bullet}. \quad (41)$$

Since  $\text{rk}(\mathbb{S}_{\bullet}) = 1$ , we now correctly predict the existence of  $\ell_{\bullet} = 3$  conservation laws. Denoting  $\mathfrak{a}_{\bullet}$  the number of emanants (emergent conservation laws), we have

$$\mathfrak{a}_{\bullet} = \ell_{\bullet} - \ell_{\circ} \quad (42)$$

The left nullvector  $\boldsymbol{\ell}_{\bullet}^{(3)} = (0, 0, \kappa_2, -\kappa_1)$  can be shown to only live in the nullspace of  $\mathbb{S}_{\bullet}$ :

$$\boldsymbol{\ell}_{\bullet} \mathbb{S}_{\bullet} = \mathbf{0}, \quad \boldsymbol{\ell}_{\bullet} \mathbb{S}_{\gg} = (\kappa_2, -\kappa_1) \neq \mathbf{0}. \quad (43)$$

Rendering reactions irreversible can thus lead to the emergence of additional conserved quantities. However, not every collinear pair of reactions supplies us with a conservation law. Let us therefore establish a rule for what additional quantities we need to count.

#### IV. EMERGENT CONSERVATION LAWS

To correctly account for conserved quantities due to collinear irreversible reactions, we need to construct a stoichiometric matrix wherein all reaction currents are linearly independent. Under mass-action, a pair of irreversible reactions is collinear if they have

the same stoichiometry in their reactants (discounting reactants fixed in concentration, i.e., chemostatted reactants[12], cf. Sec V A). Collinear reactions thus have the same column entries in the stoichiometric reactant matrix  $\nu^{\ominus}$  (cf. Eq. (8)).

Starting from  $\mathbb{S}_{\gg}$ , we merge (irreversible) collinear reactions in  $\mathbb{S}_{\gg}$  until none remain to obtain  $\mathbb{S}_{\blacktriangleright}$ , and define  $\mathbb{S}_{\bullet} = (\mathbb{S}_{\blacktriangleright}, \mathbb{S}_{\blacktriangleright}, -\mathbb{S}_{\blacktriangleright})$  as the resulting matrix. We denote with the *co-production index*  $\Upsilon$  the number of merged reactions:

$$\Upsilon = r_{\blacktriangleright} - r_{\bullet}. \quad (44)$$

We can now apply the FTLA on the difference

$$\text{rk}(\mathbb{S}_{\blacktriangleright}) - \text{rk}(\mathbb{S}_{\bullet}) = \Delta s - \Delta \ell = \Delta r - \Delta c. \quad (45)$$

where  $\Delta s = 0$ , as merging columns leaves species untouched and  $\Delta r = -\Upsilon$ . We define

$$\wedge_{\bullet} = c_{\circ} - c_{\bullet}, \quad (46)$$

and noting that  $\Delta c = \wedge_{\bullet}$ ,  $\Delta \ell = \mathfrak{a}_{\bullet}$  we obtain a form relating the counts of chemically meaningful quantities:

$$\Upsilon = \mathfrak{a}_{\bullet} + \wedge_{\bullet}, \quad (47)$$

where

$\Upsilon$ : co-production index,  $\#$  (collinear) co-production relations

$\mathfrak{a}_{\bullet}$ :  $\#$  co-production emanants (emergent conservation laws),

$\wedge_{\bullet}$ :  $\#$  broken cycles.

It follows that each collinear irreversible reaction must either produce an irreversible conservation law or lead to the loss of a previously present cycle upon merging reactions, an example for the latter is shown in Fig. 5, which is elaborated on in Sec. C.

Upon substitution, a more complete SL1 (where  $\ell$  includes co-production) would become:

$$s - \ell_{\bullet} = r_{\bullet} - c_{\bullet}, \quad (48)$$

$$s - (\ell_{\circ} + \mathfrak{a}_{\bullet}) = (r - \Upsilon) - (c_{\circ} - \wedge_{\bullet}). \quad (49)$$

However, we recall that these indices are governed by two independent relations:

$$s - \ell_{\circ} = r - c_{\circ}, \quad (50)$$

$$\Upsilon = \mathfrak{a}_{\bullet} + \wedge_{\bullet}, \quad (51)$$

With the co-production law, we are now equipped to characterize the candidate for a non-integer conservation law in Ref. [76]. This is illustrated in Fig. 4 and analyzed in detail in Sec. B of the Appendix. A co-production

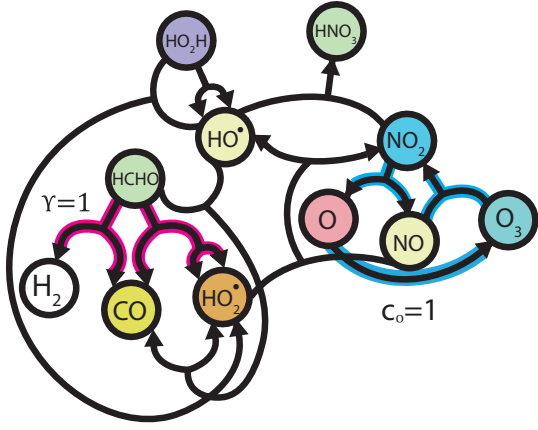


FIG. 4: An Atmospheric CRN model with co-production index  $\Upsilon = 1$ . Collinear reactions are highlighted in pink. These do not include cycle reactions - highlighted in blue - and hence no cycles break upon merging collinear reactions  $\Lambda_{\bullet} = 0$ .  $\vartheta_{\bullet} = 1$  co-production conservation law then results from the co-production law  $\Upsilon = \vartheta_{\bullet} + \Lambda_{\bullet}$ , confirming the newly found law  $CQ_3$  marks the detection of a genuine conservation law.

index  $\Upsilon = 1$  follows from visual inspection of the highlighted reactions in Fig. 4.

The collinear reactions correspond to  $r_4, r_5$  in

$$\mathbb{S}_{\triangleright} = \begin{pmatrix} 0 & 1 & -1 & 0 & 0 & 0 & 0 & 0 & 0 & 0 \\ 1 & 0 & -1 & 0 & 0 & 0 & -1 & 0 & 0 & 0 \\ -1 & 0 & 1 & 0 & 0 & 0 & 0 & 1 & -1 & 0 \\ 0 & 0 & 0 & -1 & -1 & -1 & 0 & 0 & 0 & 0 \\ 0 & 0 & 0 & 2 & 0 & 1 & -1 & 0 & 0 & 1 \\ 0 & 0 & 0 & 0 & 0 & 0 & 0 & 0 & -1 & -1 \\ 0 & 0 & 0 & 0 & 0 & -1 & 1 & -1 & 2 & -1 \\ 1 & -1 & 0 & 0 & 0 & 0 & 0 & 0 & 0 & 0 \\ 0 & 0 & 0 & 0 & 0 & 0 & 0 & 1 & 0 & 0 \\ 0 & 0 & 0 & 1 & 1 & 1 & 0 & 0 & 0 & 0 \\ 0 & 0 & 0 & 1 & 0 & 0 & 0 & 0 & 0 & 0 \end{pmatrix}$$

By merging  $r_4$  and  $r_5$ , a stoichiometric matrix  $\mathbb{S}_{\bullet}$  of independent reactions is obtained

$$\mathbb{S}_{\bullet} = \begin{pmatrix} 0 & 1 & -1 & 0 & 0 & 0 & 0 & 0 & 0 & 0 \\ 1 & 0 & -1 & 0 & 0 & 0 & -1 & 0 & 0 & 0 \\ -1 & 0 & 1 & 0 & 0 & 1 & -1 & 0 & 0 & 0 \\ 0 & 0 & 0 & -1 & -1 & 0 & 0 & 0 & 0 & 0 \\ 0 & 0 & 0 & 2p & 1 & -1 & 0 & 0 & 1 & 0 \\ 0 & 0 & 0 & 0 & 0 & 0 & 0 & 0 & -1 & -1 \\ 0 & 0 & 0 & 0 & -1 & 1 & -1 & 2 & -1 & 0 \\ 1 & -1 & 0 & 0 & 0 & 0 & 0 & 0 & 0 & 0 \\ 0 & 0 & 0 & 0 & 0 & 0 & 1 & 0 & 0 & 0 \\ 0 & 0 & 0 & 1 & 1 & 0 & 0 & 0 & 0 & 0 \\ 0 & 0 & 0 & 1-p & 0 & 0 & 0 & 0 & 0 & 0 \end{pmatrix}.$$

which leads to the emergence of a new co-production law as left nullvector:

$$\ell_{\bullet} = \left( 6, -5, 1, 3, 9, 6, 3, 6, 4, -3, \frac{6-18p}{1-p} \right). \quad (52)$$

We show in Sec. B that this is the quantity found by the SID algorithm in Ref. [76], and that Eq. (49) accounts for all true[94] conserved quantities SID may find for a CRN.

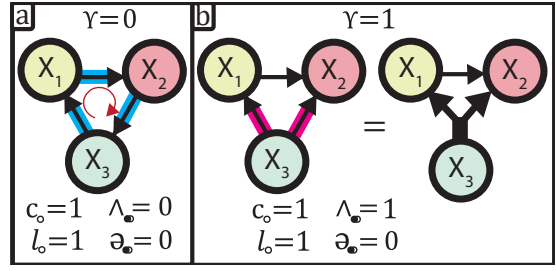


FIG. 5: a) a cyclic CRN composed of irreversible reactions. Cycle reactions are highlighted in blue. Reversing any of the reaction arrows in this cyclic CRN affords CRN b) with co-production index 1. After merging collinear reactions, the original reaction cycle can no longer be performed.

## V. BEYOND ISOBESTIC POINTS: DATA DIMENSION

To generalize the utility of isobestic points, we introduce the notion of a data dimension  $d$ . For a CRN modeled through a set of variables  $V$ , we define the model dimension  $d(V)$

$$d(V) = v - \ell(V), \quad (53)$$

$v$ : # assessed variables ( $v = |V|$ )

$\ell(V)$ : # constraints on these variables, i.e., number of conserved quantities for these variables.

In the context of a CRN described using  $s$  species variables, we have a set of variables  $X = \{[X_1], \dots, [X_s]\}$ . We retain the convention that  $s = |X|$ ,  $\ell = \ell(X)$  and thus:

$$d(X) = s - \ell. \quad (54)$$

Suppose we monitor a system spectroscopically, assuming a fixed linear relation between species and absorbance throughout the experiment (e.g., temperature is fixed and we are within the linear regime of the detector). Thus, we suppose that the Lambert-Beer law is valid

$$A_{\lambda} = L_p^{-1} \sum_{k=1}^s [X_k] \epsilon_k(\lambda), \quad (55)$$

where  $L_p$  is the light path length and we monitor in bins around  $n$  wavelengths,  $\Lambda = \{\lambda_1, \lambda_2, \dots, \lambda_n\}$ ,

$$d_t \mathbf{A}(\Lambda) = L_p^{-1} \mathbb{S} \mathbf{J} \mathbf{E}(\Lambda), \quad (56)$$

so that  $\mathbf{E}$  is an  $s$ -by- $n$  matrix with each row corresponding to the spectrum of a species:

$$\mathbf{E} = \begin{pmatrix} \epsilon_1(\lambda_1) & \epsilon_1(\lambda_2) & \dots & \epsilon_1(\lambda_n) \\ \epsilon_2(\lambda_1) & \epsilon_2(\lambda_2) & \dots & \epsilon_2(\lambda_n) \\ \vdots & \vdots & \ddots & \vdots \\ \epsilon_s(\lambda_1) & \epsilon_s(\lambda_2) & \dots & \epsilon_s(\lambda_n) \end{pmatrix}. \quad (57)$$

The rank of  $\mathbb{E}$  is at most  $s$ , when all species are spectroscopically distinct and  $n$  is sufficiently large to discern them. We consider the following contributions that lower the rank

$$\text{rk}(\mathbb{E}(\Lambda)) = s - s_{\blacksquare}(\Lambda) - \S(\Lambda) - \ell_{\parallel}(\Lambda). \quad (58)$$

$s_{\blacksquare}(\Lambda)$  : # concealed species, species not measurably absorbing in  $\Lambda$

$\S(\Lambda)$  : isospectral index, # independent pairs of isospectral species in  $\Lambda$  (e.g., enantiomers in achiral environments)

$\ell_{\parallel}(\Lambda)$  : # further collinearities among absorption spectra in  $\Lambda$

Further collinearities ( $\ell_{\parallel}(\Lambda)$ ) can occur when  $n$  becomes comparable to the dimension. For instance, when computer vision is used for reaction monitoring[95–97], the RGB images have  $n = 3$ , which may set an upper bound on the dimension that may be resolved.

For the data dimension for  $n = |\Lambda|$  spectral variables we write Eq.(53) as

$$d(\Lambda) = n - \ell(\Lambda) \leq d(\mathbb{X}). \quad (59)$$

Let us denote the number of dimensions not accounted for spectroscopically as  $\Delta d_{\Lambda}$

$$d(\mathbb{X}) - d(\Lambda) = \Delta d_{\Lambda}. \quad (60)$$

### A. The concealed species law versus chemostatting

Next, we consider the subnetwork we effectively see due to the first two constraints in Eq. 58 relating species to their spectral observables. First, we partition  $\mathbb{S}$  in a matrix  $\mathbb{S}_{\square}$  of species that absorb, and a matrix  $\mathbb{S}_{\blacksquare}$  of species that do not:

$$\mathbb{S} = \begin{pmatrix} \mathbb{S}_{\blacksquare} \\ \mathbb{S}_{\square} \end{pmatrix}, \quad (61)$$

from applying the FTLA / SL1 to  $\mathbb{S}_{\blacksquare}$ , we obtain

$$s_{\blacksquare}(\Lambda) = b_{\square}(\Lambda) + a_{\square}(\Lambda), \quad (62)$$

$$b_{\square}(\Lambda) = \ell - \ell_{\square} \quad (63)$$

$$a_{\square}(\Lambda) = c_{\square} - c \quad (64)$$

$b_{\square}(\Lambda)$ : # concealed conservation laws in visible subnetwork ( $\mathbb{S}_{\square}$ )

$a_{\square}(\Lambda)$ : # apparent cycles in visible subnetwork

We borrow this partitioning procedure [12] from a different context, in which  $s_Y$  species are chemostatted (fixed in concentration),

$$\mathbb{S} = \begin{pmatrix} \mathbb{S}_Y \\ \mathbb{S}_X \end{pmatrix}, \quad (65)$$

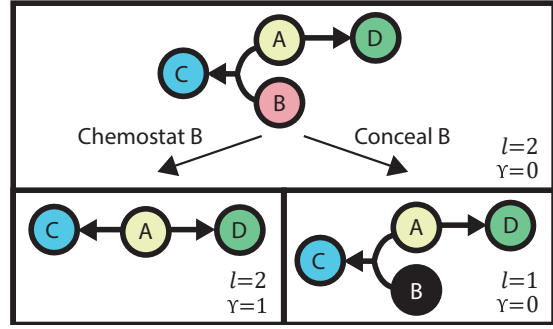


FIG. 6: Contrasting chemostatting and concealing. Upon fixing concentration  $[B] = cte$ ,  $r_1$  and  $r_2$  become collinear, and we obtain a co-production index  $\Upsilon = 1$ . Upon concealing  $[B]$ , it remains a variable, but we lose access to it. Reactions  $r_1$  and  $r_2$  then remain independent.

and then

$$s_Y = b_X + a_X, \quad (66)$$

$$b_X = \ell - \ell_X, \quad (67)$$

$$a_X = c_X - c. \quad (68)$$

$b_X$ : # broken conservation laws in  $\mathbb{S}_X$ ,  
 $a_X$ : # emergent cycles in internal network.

An emergent cycle  $\mathbf{a}$  denotes a right nullvector of the subnetwork with fewer species that does not extend to the full network

$$\mathbb{S} \mathbf{a}_{\square} \neq \mathbf{0}, \quad \mathbb{S}_{\square} \mathbf{a}_{\square} = \mathbf{0}, \quad (69)$$

$$\mathbb{S} \mathbf{a}_X \neq \mathbf{0}, \quad \mathbb{S}_X \mathbf{a}_X = \mathbf{0}. \quad (70)$$

However, the net effect of chemostatting species is not equivalent to concealing them: previously independent irreversible reactions can become collinear by fixing variables (chemostatting), but not by concealing variables. A minimal example is given in Fig. 6. The same phenomenon occurs in the example provided in Appendix B.

### B. The isospectral species law

In the observable subnetwork  $\mathbb{S}_{\square}$ , we now merge all pairs of isospectral species that measurably absorb, to describe the effective subnetwork due to their indistinguishability. We denote as  $\S(\Lambda)$  the number of mergers thus performed.

$$\text{rk}(\mathbb{S}_{\square}) - \text{rk}(\mathbb{S}_{\blacklozenge}) = \Delta s - \Delta \ell = \Delta r - \Delta c, \quad (71)$$



for which  $\Delta s = \S(\Lambda)$ . Reactions that vanish by merging a pair of species are reactions appearing as direct isomerization reactions in  $\mathbb{S}_{\square}$ ,  $\Delta r = r_{\sim}$ . Merging isospectral species can either break conservation laws or create apparent cycles, affording the isospectral species law

$$\S(\Lambda) = b_{\S}(\Lambda) + a_{\S}(\Lambda) + r_{\sim}(\Lambda), \quad (72)$$

where

$b_{\S}(\Lambda)$  : # lost conservation laws

$a_{\S}(\Lambda)$  : # apparent cycles (combinations of reactions that leave discernable variables unchanged)

$r_{\sim}(\Lambda)$  : # direct isomerization reactions among isospectral species pairs

We can then express the loss of dimension between the full CRN and what is discerned spectroscopically as

$$\Delta d_{\Lambda} = \S(\Lambda) + s_{\blacksquare}(\Lambda) - r_{\sim}(\Lambda) - b_{\square}(\Lambda) - b_{\S}(\Lambda) \quad (73)$$

$$= a_{\square}(\Lambda) + a_{\S}(\Lambda). \quad (74)$$

We can represent these spectral properties in network representations, and thereby graphically determine  $d(X)$  and  $d(\Lambda)$ . Some examples are provided in Fig. 7. More examples with elaboration are provided in Sec. D.

The dimension of spectroscopic data can match the original data dimension  $d(X)$  ( $\Delta d_{\Lambda} = 0$ ) even if not all species are discernable. Up to  $\ell$  variables can be lost (Eq.(73)), provided this only leads to unobservable conservation laws or isospectral isomerization reactions. Conversely, each missing dimension corresponds to an apparent cycle, i.e., combinations of reactions that leave the discernable variables unchanged (this includes reactions which have become unobservable  $\blacksquare \rightleftharpoons \blacksquare$ ). For nonabsorbing species, such a cycle requires two chemostats ( $s_{\blacksquare}(\Lambda) \geq 1$ ) for the effective CRN. Hence, for  $s_{\blacksquare}(\Lambda) = 1$ , no loss of dimension occurs.

## VI. MEASURING DATA DIMENSION

We will now formalize the process of measuring the data dimension. We define a spectral data matrix  $\mathbb{A}$  as the matrix containing spectra measured at successive times  $t_1, t_2, \dots, t_m$

$$\mathbb{A} = \begin{pmatrix} A_{\lambda_1}(t_1) & A_{\lambda_2}(t_1) & \dots & A_{\lambda_n}(t_1) \\ A_{\lambda_1}(t_2) & A_{\lambda_2}(t_2) & \dots & A_{\lambda_n}(t_2) \\ \vdots & \vdots & \ddots & \vdots \\ A_{\lambda_1}(t_m) & A_{\lambda_2}(t_m) & \dots & A_{\lambda_n}(t_m) \end{pmatrix}. \quad (75)$$




CRN	$d(X)$	$d(\Lambda)$	$s_{\blacksquare}$	$b_{\square}$	$a_{\square}$	$\S$	$b_{\S}$	$a_{\S}$	$r_{\sim}$
	2	1	0	0	0	1	0	1	0
	2	1	0	0	0	1	0	1	1
	3	2	3	2	1	0	0	0	0
	3	3	2	2	0	0	0	0	0

FIG. 7: Illustration of laws for isospectral (Eq. (72)) and concealed (Eq. (62)) species for several CRNs. Dark nodes correspond to spectroscopically inactive species. Species that are indistinguishable are marked with a star. New cycles - leading to loss of data dimension - are highlighted in orange and blue. Data dimensions:  $d(X), d(\Lambda)$  (spectral),  $d(X)$  (species).  $d(\Lambda)$  spectral data dimension,  $s_{\blacksquare}(\Lambda)$  : # concealed species,  $b_{\square}(\Lambda)$  : # concealed conservation laws,  $a_{\square}(\Lambda)$  : # apparent cycles,  $\S(\Lambda)$  : isospectral index,  $r_{\sim}(\Lambda)$  : # isospectral isomerization reactions,  $b_{\S}(\Lambda)$  : # isospectral broken conservation laws,  $a_{\S}(\Lambda)$  #, isospectral emergent cycles.

We denote by  $\Delta A_{\lambda_n}$  a mean subtracted absorption

$$\Delta A_{\lambda_n}(t_q) = A_{\lambda_n}(t_q) - \frac{1}{m} \sum_{k=1}^m A_{\lambda_n}(t_k), \quad (76)$$

and we analogously define

$$\Delta \tilde{\mathbb{A}} = \begin{pmatrix} \Delta A_{\lambda_1}(t_1) & \Delta A_{\lambda_2}(t_1) & \dots & \Delta A_{\lambda_n}(t_1) \\ \Delta A_{\lambda_1}(t_2) & \Delta A_{\lambda_2}(t_2) & \dots & \Delta A_{\lambda_n}(t_2) \\ \vdots & \vdots & \ddots & \vdots \\ \Delta A_{\lambda_1}(t_m) & \Delta A_{\lambda_2}(t_m) & \dots & \Delta A_{\lambda_n}(t_m) \end{pmatrix}. \quad (77)$$

To contrast with genuine (noisy) data, we let  $\Delta \tilde{\mathbb{A}}$  derive from an exact (noise-free) solution  $[\mathbf{X}](t)$  to the dynamics multiplied by exact theoretical spectra. Whereas we expect a true data matrix to be of full rank, noise-free  $\Delta \tilde{\mathbb{A}}$  can have a nonzero kernel, and (starting away from equilibrium) its rank is given by the spectroscopic data dimension  $d(\Lambda)$

$$\text{rk}(\Delta \tilde{\mathbb{A}}) = d(\Lambda). \quad (78)$$

We can then model noisy data by addition of a random matrix  $\eta$  whose entries are independent identically distributed random variables with mean 0 and variance  $\epsilon^2$

$$\Delta \mathbb{A} = \Delta \tilde{\mathbb{A}} + \eta(\epsilon), \quad (79)$$

so that almost always

$$\text{rk}(\mathbb{A}) = \text{rk}(\eta) = \max(n, m). \quad (80)$$

While we cannot directly assess  $d(\Lambda)$ , we can adopt a decomposition procedure to attempt to separate signal-rich dimensions from noisy ones, and estimate a dimension  $d_\epsilon$  from that by some criterion. A simple criterion introduced in Sec. VI A considers the spectral properties of random matrix [98]  $\eta(\epsilon)$  and will suffice for our examples (see Refs.[99–101] for more thorough considerations). We will call the estimate  $d_\epsilon(\Lambda)$  hereby obtained the discernable dimension.

The procedure we will use for our illustration is singular value decomposition (SVD), which decomposes the data in successive components that maximally explain remaining variance (alternative decompositions to estimate data dimension exist[64]). The SVD has several desirable mathematical properties and is widely implemented. A disadvantage in our context is that the decomposition is not tailored to the structure of our problem, and is prone to underestimating  $d(\Lambda)$  when dimensions become small.

The need for  $d_\epsilon(\Lambda)$  becomes apparent by revisiting the CRN  $C \rightleftharpoons A + B \rightleftharpoons D$ , starting with only A, B ( $[A]_0, [B]_0 > 0, [C]_0, [D]_0 = 0$ ). Up to a linear approximation, we then have

$$\begin{aligned} \Delta[A] &= -(k_1 + k_2) [A]_0 [B]_0 t + \mathcal{O}(t^2), \\ \Delta[C] &= -k_1 [A]_0 [B]_0 t + \mathcal{O}(t^2), \\ \Delta[D] &= -k_2 [A]_0 [B]_0 t + \mathcal{O}(t^2). \end{aligned}$$

For a signal-to-noise ratio  $\epsilon > 0$ , we can then choose a sufficiently small time  $t^*$  such that higher order corrections starting at  $\mathcal{O}(t^2)$  become comparable to noise. For data recorded on shorter timescales, we cannot yet distinguish reverse reactions, and then  $C \rightleftharpoons A + B \rightleftharpoons D$  behaves as  $C \leftarrow A + B \rightarrow D$ , i.e., we have a discernable dimension  $d_\epsilon(X) = 1$  for  $t \ll t^*$ ,  $d_\epsilon(X) = 2$  for  $t \gg t^*$ . Under such circumstances, a co-production law  $\mathfrak{a}_\bullet$  may be transient.

Resolution and chemical interpretations of missing dimensions  $d_0 - d_\epsilon$  is outside the scope of this paper and will be discussed in our follow-up work. For the remaining examples, we confine our discussions to cases where no dimensions are lost due to resolution, i.e.,  $\epsilon$  is chosen such that  $d_\epsilon(\Lambda) = d_0(\Lambda) = d(\Lambda)$ .

### A. SVD for spectral data

A singular value decomposition of the  $m$ -by- $n$  matrix  $\Delta\mathbb{A}$  represents it as a product of

three matrices

$$\Delta\mathbb{A} = U\Sigma V^T. \quad (81)$$

In our context,  $V$  is an  $n$ -by- $m$  matrix with rows  $v_1(\lambda), v_2(\lambda), \dots, v_m(\lambda)$  (right singular vectors) corresponding to spectra

$$V = \begin{pmatrix} v_1(\lambda_1) & v_2(\lambda_1) & \dots & v_m(\lambda_1) \\ v_1(\lambda_2) & v_2(\lambda_2) & \dots & v_m(\lambda_2) \\ \vdots & \vdots & \ddots & \vdots \\ v_1(\lambda_n) & v_2(\lambda_n) & \dots & v_m(\lambda_n) \end{pmatrix} \quad (82)$$

$U$  is an  $m$ -by- $m$  matrix with rows  $u_1(t), u_2(t), \dots, u_m(t)$  (left singular vectors) corresponding to time trajectories, i.e., time-dependent spectral contributions

$$U = \begin{pmatrix} u_1(t_1) & u_2(t_1) & \dots & u_m(t_1) \\ u_1(t_2) & u_2(t_2) & \dots & u_m(t_2) \\ \vdots & \vdots & \ddots & \vdots \\ u_1(t_m) & u_2(t_m) & \dots & u_m(t_m) \end{pmatrix}. \quad (83)$$

Singular vectors thus produced are orthonormal

$$UU^T = I, \quad VV^T = I. \quad (84)$$

The contributions of the singular vectors to the data are weighed by singular values  $\sigma_1, \dots, \sigma_n$ , which occur diagonally in the  $n$ -by- $m$  matrix  $\Sigma$ ,

$$\begin{aligned} \Sigma_{ki} &= \delta_i^k \sigma_k, \\ \sigma_i &= \Sigma_{ii} \geq 0, \quad \sigma_i \geq \sigma_{i+1}. \end{aligned} \quad (85)$$

Singular values are non-negative and placed in decreasing order. Based on the results of SVD, a single spectrum at time  $t_q$  can now be reconstituted as

$$A_\lambda(t_q) = \sum_i^{\min(n, m)} \sigma_i u_i(t_q) v_i, \quad (87)$$

which, on the level of the data matrix  $\Delta\mathbb{A}$ , can be written as a sum of rank-1 matrices

$$\Delta\mathbb{A} = \sum_i \Delta\mathbb{A}^{(i)}, \quad (88)$$

$$\Delta\mathbb{A}^{(i)} = \sigma_i \mathbf{u}_i \mathbf{v}_i^T, \quad (89)$$

$$\text{rk}(\Delta\mathbb{A}^{(i)}) = 1. \quad (90)$$

and by truncating at  $k$  we can now approximate the data with data of rank  $k$ .

Since  $\sigma_i \geq \sigma_{i+1}$ , the reconstructive contribution of successive  $\Delta\mathbb{A}^{(i)}$  diminish with increasing  $i$ . Informed by the spectral properties of random matrix[98]  $\eta(\epsilon)$ , and supposing  $n > m$  we will consider a threshold

$$\sigma^* = \epsilon \left( 1 + \sqrt{\frac{m}{n}} \right)^2 \sqrt{m}, \quad (91)$$

We then let the discernable dimension  $d_\epsilon$  be the number of singular values above this threshold. For our examples,  $d_\epsilon(\Lambda)$  will also be qualitatively evident from visual inspection.

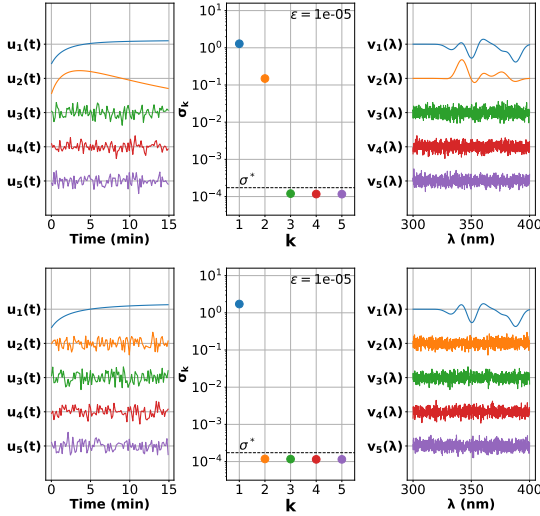


FIG. 8: (top) First 5 components of Singular value Decomposition of  $\Delta A$  for CRN  $C \rightleftharpoons A + B \rightleftharpoons D$ . By visual inspection, only 2 non-noisy trajectories and spectra are discerned, consistent with  $d_\epsilon(\Lambda) = 2$ . (bottom) First 5 components of Singular Value Decomposition of  $\Delta A$  for CRN  $C \leftarrow A + B \rightarrow D$ .  $d_\epsilon(\Lambda) = 1$ .  $v_1(\lambda)$  crosses the origin 4 times, corresponding to 4 isosbestic points in Fig. 1. For both, we have noise level  $\epsilon = 10^{-5}$ ,  $m = 100$  successive spectra,  $n = 1000$  wavelengths.

### 1. Beyond isosbestic points

Provided small enough  $\epsilon$ , signal is captured within the first  $d(\Lambda)$  components, and further dimensions should look qualitatively distinct. Fig. 8 shows the first 5 components for the spectral data for our initial example in Fig. 1 ( $d(\Lambda) = 2$ )

An analysis that makes use of the whole spectrum (such as SVD) allows for a more robust identification of a dimension compared to the use of special features such as isosbestic points or isosbestic lines.

As will be developed in more detail in paper II, a CRN may have  $d(\Lambda) = 1$  but inherently not yield an isosbestic point, for instance when we are looking at single reactions of the form



or



where the spectral change due to consumption (resp. production) is not counterbalanced, i.e. there is no positive conservation law. (on SVD, the corresponding  $v_1(\lambda)$  will not change in sign).

## VII. DISCUSSION

Machine learning (ML) approaches can learn representations of chemical data and make predictions based on this representation. Importantly, any ML representation that incorporates inherent symmetries and constraints will make more physically sound predictions and will need less training data[102]. The algorithmic detection of such symmetries has become an important development in its own right[76, 89, 103–106]. Understandably, many ML approaches have adopted CRNs as the model representation to be learned, through a variety of learning strategies [107–110]. The challenges posed by ML and MCR thus bring us back to our original unresolved challenge, namely, how CRN structure follows from data, and *vice versa*.

In paper I, we advance a first line of results to relate structural elements (cycles, conservation laws, reactions, species, co-production) in the CRN to the dimension of the data it can bring forth. We have by no means exhausted this strategy: further dimensional quantities (such as isosbestic points and its generalizations, data dimensions with added constraints) can be defined and measured, and related to structural elements by the fundamental theorem of linear algebra. This will form the object of paper II and III.

The data dimension is useful for filtering competing hypotheses. As more measured dimensional quantities (such as data dimension  $d$ ) are combined, the identity of a CRN can be narrowed down further: the pool of CRNs that can obey all the observed constraints shrinks exponentially with the number of constraints.

For our laws to pertain to as much data as possible recorded in experimental practice, we derived laws pertaining to the common chemical experimental context in which not all species can be observed or distinguished. Further consideration of the viewpoint of an observer[111] should be beneficial for CRNs in theory and experiment, as it has been for other physical theories.

### VIII. CONCLUSION

We characterized effects of irreversible reactions and concealed species on the dimension of chemical data. This furnished several new CRN laws, which fundamentally derive from applying the first structural law (SL1)  $s - \ell = r - c$  to new contexts: irreversible co-production and incomplete observation (through spectroscopy). The reinterpretation of underlying arguments in this new context in terms of countable chemically meaningful concepts thereby leads to laws of chemistry that govern it.

The co-production law  $\Upsilon = \ominus_{\bullet} + \wedge_{\bullet}$  formalizes one of the prominent topological differences that can arise in passing from CRNs with reactions that are reversible to ones that are irreversible. A set of common conservation laws can be found from an analysis of integer stoichiometry, but irreversible CRNs can have further (non-integer) conservation laws that such an analysis would miss. Conversely, conservation laws are more informative of CRN structure than currently considered, as they pick up on more structural detail. This provides further motivation to extract them from chemical data and to elucidate how that can be done.

Critically, data one collects in chemistry (e.g., by UV-VIS) often need not 'see' all underlying CRN species. A dimensional theory for chemical data must thus account for the effects of what can and cannot be experimentally observed, and what cannot be distinguished. Within the scope of this work, these effects are governed by the concealed species law  $s_{\blacksquare}(\Lambda) = b_{\square}(\Lambda) + a_{\square}(\Lambda)$  and isospectral species law  $\S(\Lambda) = b_{\S}(\Lambda) + a_{\S}(\Lambda) + r_{\sim}(\Lambda)$ . We thereby have started establishing bridges between data dimension and underlying CRN features, e.g., independent isobestic points correspond to single reactions with associated conservation law(s).

Our approach lays the foundation towards a CRN-level theory that characterizes the multifarious types of ambiguities and indeterminacies in chemical data and establishes chemical laws that govern them. By construction, such a theory provides deeper insights into the structure and chemical context of the ambiguity problem, the central problem in multivariate curve resolution (MCR). We surmise that this additional structure and context may be leveraged by a new generation of MCR algorithms and data collection protocols.

Importantly, our approach enables new inference methods by which portions of a reaction network are deduced from dimensions of portions of data, similar to how portions of NMR

spectra illuminate portions of a molecular structure. Understanding how structure in chemistry introduces structure in data thereby creates new tools allowing to address greater analytical challenges in chemistry.

### Appendix A: Glossary

In the context of a recently started effort to clarify and harmonize concepts and notation in stochastic thermodynamics, we clarify below the notation and conventions that have been adopted.[25] Our notation closely follows the notation adopted in the framework of Ref [12], and the proposed unified notation from the (post)modern thermodynamics lecture notes [25], with the following exceptions:

- Stoichiometric matrices are denoted by  $\mathbb{S}$
- Rate constants are denoted by  $\kappa$  (reserving  $k$  for indices).

We adopt the following additional conventions:

- For sub/superscripts not used as integer indices, non-alphanumeric symbols ( $\circ$ ,  $\blacksquare$ ,  $\triangleright$ ) are preferred.
- Non-alphanumeric sub/superscripts are chosen that have some relation to the context. E.g. equivalence  $\sim$  for isomers, a black box  $\blacksquare$  for a concealed subnetwork, etc.
- Fillable sub/superscripts are preferred when decompositions will be taken (e.g.  $\square$ ,  $\triangleright$ ,  $\circ$ .)

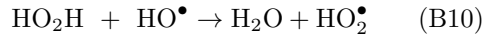
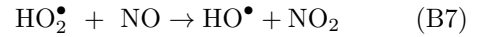
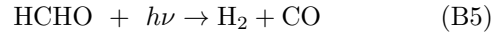
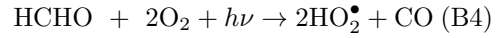
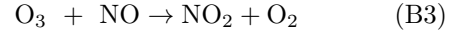
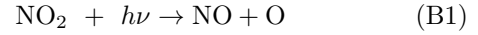
Symbol	Meaning	First appearance
<b>Stoichiometric matrices (<math>\mathbb{S}, \nu, \mathbb{P}</math>)</b>		
$\mathbb{S}$	regular $\mathbb{S}$	p.4 Eq.(8)
$\nu^{\oplus}$	$\mathbb{S}$ , positive part	p.4, Eq.(8)
$\nu^{\ominus}$	$\mathbb{S}$ , negative part	p.4, Eq.(8)
$\mathbb{S}_{\circ}$	all reactions once	p.4 Eq.(11)
$\mathbb{S}_{\bowtie}$	reversible reactions	p.5 Eq.(22)
$\mathbb{S}_{\triangleright}$	irreversible reactions	p.5 Eq.(22)
$\mathbb{S}_{\gg}$	all reactions, irreversible reactions twice	p.5 Eq.(23)
$\mathbb{S}_{\bullet}$	merged co-production	p.6 Eq. (40)
$\mathbb{S}_{\Upsilon}$	external subnetwork	p.8 Eq. (65)
$\mathbb{S}_{\chi}$	internal subnetwork	p.8 Eq. (65)
$\mathbb{S}_{\blacksquare}$	concealed subnetwork	p.8 Eq. (61)
$\mathbb{S}_{\square}$	absorbing subnetwork	p.8 Eq. (61)
$\mathbb{S}_{\blacklozenge}$	merged isospectral species	p.9, Eq. (71)
<b>species (<math>s</math>)</b>		
$s$	# species	p.4 Eq.(15)
$s_{\blacksquare}(\Lambda)$	# concealed species	p.8 Eq. (58)
$s_{\Upsilon}$	# chemostats	p.8, Eq.(68)

Symbol	Meaning	First appearance
reactions ( $r, \Upsilon$ )		
$r$	# reactions	p.4 Eq.(15)
$r_{\triangleright}$	# irreversible reactions	p.5 Eq.(24)
$r_{\triangleright\triangleright}$	# reactions, counting reversibility twice	p.5 Eq.(24)
$r_{\circ}$	# reactions, counting reversibility once	p.5 Eq.(24)
$r_{\boxtimes}$	# reversible reactions	p.5 Eq.(25)
$\Upsilon$	Co-production index	p.6 Eq. (43)
$r_{\sim}(\Lambda)$	# independent direct isomerization reactions among isospectral species	p.9 Eq.(72)
conserved quantities ( $\ell, b$ )		
$\ell$	# conserved quantities	p.4 Eq.(15)
$\ell_{\circ}$	# conserved quantities, $\mathbb{S}_{\circ}$	p.4 Eq.(24)
$\mathfrak{a}_{\bullet}$	# Co-production emanants, Co-production conservation laws	p.5 Eq. (40)
$\ell_{  }(\Lambda)$	# further collinearities in absorption spectra	p.8 Eq. (58)
$b_{\square}(\Lambda)$	# concealed conservation laws	p.8 Eq. (62)
cycles ( $c, \Lambda, a$ )		
$c_{\circ}$	# cycles, reversible CRN	p.4 Eq.(24)
$c$	# cycles	p.4 Eq.(15)
$\wedge_{\bullet}$	# broken cycles due to co-production	p.6 Eq. (47)
$a_{\square}(\Lambda)$	# apparent cycles	p.8 Eq. (62)
dimension indices ( $d, I, \S$ )		
$d$	data dimension	p.7 Eq. (53)
$\Delta d_{\Lambda}$	# CRN dimensions missing in spectroscopic data	p.9 Eq. (60)
$\S(\Lambda)$	Isospectral index	p. Eq. (58)
other indices		
$A_{\lambda}$	absorbance	p.7 Eq. (55)
$L_p$	path length	p.7 Eq. (55)
$[X_k]$	amount concentration	p.7 Eq. (55)
$\epsilon_k(\lambda)$	molar extinction coefficient	p.7 Eq. (55)
$\mathbb{E}(\Lambda)$	Molar Extinction Matrix	p. Eq. (57)

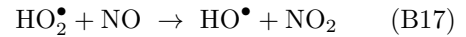
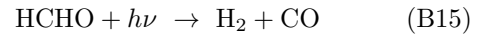
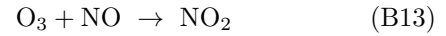
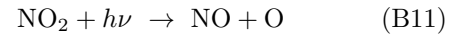
### Appendix B: A hidden conserved quantity in an atmospheric chemistry model

As a final application example, we revisit the atmospheric model considered in recent studies[76, 89], in which a non-integer quantity that appeared to be conserved was discovered numerically. It was unclear whether this was an approximate conservation law, or a genuine one, and no clear interpretation could be given for its non-integer nature. We address both questions below by showing that it is an instance of co-production conservation.

The model starts by considering the irreversible reactions



It is further supposed that  $\text{H}_2\text{O}$  is not monitored, and that  $\text{O}_2$  is a reservoir species (chemostatted). The subnetwork thus afforded is



Since  $\text{H}_2\text{O}$  only occurs as a sink species, the effects of concealing it and chemostatting it are equivalent ( $b_X = 1$  or  $b_{\square} = 1$ ).

We will now see how coproduction emerges: we remove  $\text{O}_2$  and  $\text{H}_2\text{O}$  from the description by chemostatting. By the chemostatting of  $\text{O}_2$ , reactions  $r_4$  and  $r_5$  have become collinear, hence  $\Upsilon = 1$ . The chemostat law (i.e., Eq. (68)) states that  $s^Y = 2$  reservoirs are introduced, and here one can readily check that  $b = 2$  stoichiometric conservation laws are broken (i.e., hydrogen and oxygen conservation being lost). Since  $\mathfrak{a}_{\bullet} = 1$ , the number of conservation laws is only reduced by 1 rather than 2. The subnetwork with the highlighted collinear reactions is depicted in Fig. 4.

The subnetwork satisfies  $\mathbb{S}_{\triangleright\triangleright} = \mathbb{S}_{\triangleright}$ , with stoichiometric matrix

$$\mathbb{S}_{\triangleright} = \begin{pmatrix} 0 & 1 & -1 & 0 & 0 & 0 & 0 & 0 & 0 & 0 \\ 1 & 0 & -1 & 0 & 0 & 0 & -1 & 0 & 0 & 0 \\ -1 & 0 & 1 & 0 & 0 & 0 & 1 & -1 & 0 & 0 \\ 0 & 0 & 0 & -1 & -1 & -1 & 0 & 0 & 0 & 0 \\ 0 & 0 & 0 & 2 & 0 & 1 & -1 & 0 & 0 & 1 \\ 0 & 0 & 0 & 0 & 0 & 0 & 0 & 0 & -1 & -1 \\ 0 & 0 & 0 & 0 & 0 & -1 & 1 & -1 & 2 & -1 \\ 1 & -1 & 0 & 0 & 0 & 0 & 0 & 0 & 0 & 0 \\ 0 & 0 & 0 & 0 & 0 & 0 & 1 & 0 & 0 & 0 \\ 0 & 0 & 0 & 1 & 1 & 1 & 0 & 0 & 0 & 0 \\ 0 & 0 & 0 & 0 & 1 & 0 & 0 & 0 & 0 & 0 \end{pmatrix}$$

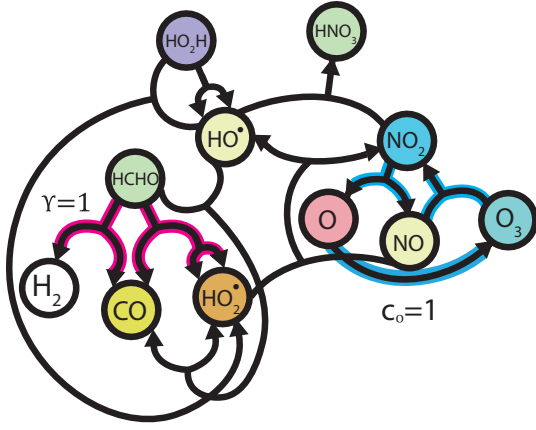


FIG. 9: Figure 4, reproduced for convenience. An Atmospheric CRN model with co-production index  $\Upsilon = 1$ . Collinear reactions are highlighted in pink. These do not include cycle reactions - highlighted in blue - and, hence, no cycles break upon merging collinear reactions  $\wedge_{\bullet} = 0$ .  $\mathfrak{a}_{\bullet} = 1$  co-production conservation law then results from the co-production law  $\Upsilon = \mathfrak{a}_{\bullet} + \wedge_{\bullet}$ , confirming the newly found law  $CQ_3$  marks the detection of a genuine conservation law.

$$(B21)$$

Which has  $\text{rk}(\mathbb{S}_{\triangleright}) = 9$ . Since  $r_{\triangleright} = 10$ , there is  $c_{\circ} = 1$  cycle, involving  $r_1$  to  $r_3$

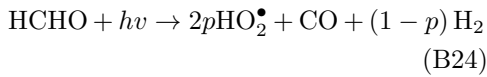
$$\mathbf{c} = (1, 1, 1, 0, 0, 0, 0, 0, 0, 0) \quad (B22)$$

which is highlighted in Fig. 9.

As reactions  $r_4$  and  $r_5$  are now collinear, we merge them

$$pr_4 + (1-p)r_5, \quad p = \frac{k_4}{k_4 + k_5} \quad (B23)$$

which becomes



So that our stoichiometric matrix  $\mathbb{S}_{\bullet}$  in terms of independent reactions becomes

$$\mathbb{S}_{\bullet} = \begin{pmatrix} 0 & 1 & -1 & 0 & 0 & 0 & 0 & 0 & 0 & 0 \\ 1 & 0 & -1 & 0 & 0 & -1 & 0 & 0 & 0 & 0 \\ -1 & 0 & 1 & 0 & 0 & 1 & -1 & 0 & 0 & 0 \\ 0 & 0 & 0 & -1 & -1 & 0 & 0 & 0 & 0 & 0 \\ 0 & 0 & 0 & 2p & 1 & -1 & 0 & 0 & 0 & 1 \\ 0 & 0 & 0 & 0 & 0 & 0 & 0 & 0 & -1 & -1 \\ 0 & 0 & 0 & 0 & -1 & 1 & -1 & 2 & -1 & 0 \\ 1 & -1 & 0 & 0 & 0 & 0 & 0 & 0 & 0 & 0 \\ 0 & 0 & 0 & 0 & 0 & 0 & 0 & 1 & 0 & 0 \\ 0 & 0 & 0 & 1 & 1 & 0 & 0 & 0 & 0 & 0 \\ 0 & 0 & 0 & 1-p & 0 & 0 & 0 & 0 & 0 & 0 \end{pmatrix}.$$

As we have not merged any cycle reactions, no cycles are lost  $\wedge_{\bullet} = 0$ . This is readily seen by making the cycle vector  $\mathbf{c}$  one reaction shorter

$$\mathbf{c}_{\bullet} = (1, 1, 1, 0, 0, 0, 0, 0, 0, 0), \quad (B25)$$

$$\mathbb{S}_{\bullet}\mathbf{c}_{\bullet} = \mathbf{0}. \quad (B26)$$

Thus, co-production  $\Upsilon = 1$  then yields  $\mathfrak{a}_{\bullet} = 1$ , as evidenced by an additional left nullvector

$$\boldsymbol{\ell}_{\bullet}^{(3)} = \left( 6, -5, 1, 3, 9, 6, 3, 6, 4, -3, \frac{6-18p}{1-p} \right) \quad (B27)$$

To see if this is the elusive hidden conservation law[112]  $CQ_3$  reported in the literature[76], we substitute ( $p = 0.40541\dots$ ):

$$\begin{aligned} \boldsymbol{\ell}_{\bullet}^{(3)} &= (6, -5, 1, 3, 9, 6, 3, 6, 4, -3, 2.18\dots) \\ CQ_3 &\approx (6, -5, 1, 3, 9, 6, 3, 6, 4, -3, 2.21) \end{aligned}$$

The numerical estimate of the measured quantity  $CQ_3$  thus closely approximates the genuine conservation law. We can thus confirm that the observation of  $CQ_3$  was due to a genuine conserved quantity in the (chemostatted) model. The existence and exact nature - co-production conservation - of this conservation law has thereby been clarified.

In general, the SID algorithm proposed in that work[76] detects conservation laws of first order differential equations  $d_t\mathbf{x} = \mathbf{f}(\mathbf{x})$  by creating a list of  $K$  independent phase-space functions  $\mathbf{b} = b^{(1)}(\mathbf{x}), \dots, b^{(K)}(\mathbf{x})$ .  $H(\mathbf{x}) = \boldsymbol{\theta}^T \mathbf{b}(\mathbf{x})$  is then a conserved quantity, if, for all  $\mathbf{x}$ : [113]

$$g(\mathbf{x})^T \boldsymbol{\theta} = 0, \quad (B28)$$

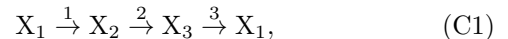
$$g(\mathbf{x}) = \nabla \mathbf{b} \mathbf{f}(\mathbf{x}). \quad (B29)$$

Applied to CRNs where  $\mathbf{x} = [\mathbf{X}]$ ,  $\mathbf{f}(\mathbf{x}) = \mathbb{S}\mathbf{J}$  and with a list of candidate functions  $\mathbf{b} = [\mathbf{X}]$ , the above equation reduces to (the transpose of) the condition  $\boldsymbol{\ell}^T \mathbb{S}\mathbf{J} = 0$  mentioned before. We conclude that the analysis provided herein is sufficient to explain all true linear conservation laws the SID algorithm might find in a CRN. There can be further conservation laws due to special choices of parameters (Sec. E).

### Appendix C: Example: $\wedge_{\bullet}$ vs $\mathfrak{a}_{\bullet}$

Coproduction can result in an emergent conservation law or a broken cycle. Here we illustrate a minimal example of a broken cycle.

For this, we first start with a CRN displaying the cycle to be broken



for which

$$\mathbb{S}_\bullet = \begin{pmatrix} -1 & 0 & 1 \\ 1 & -1 & 0 \\ 0 & 1 & -1 \end{pmatrix}. \quad (\text{C2})$$

Here, there are no reactions to be merged, and so  $\Upsilon = \mathfrak{a}_\bullet = \Lambda_\bullet = 0$ . Furthermore, there is  $c = 1$  cycle and  $\ell_o = 1$  conservation law

$$\mathbf{c} = (1, 1, 1)^T \quad (\text{C3})$$

$$L^{(1)} = [X_1] + [X_2] + [X_3] \quad (\text{C4})$$

Reversing any of the reactions will yield

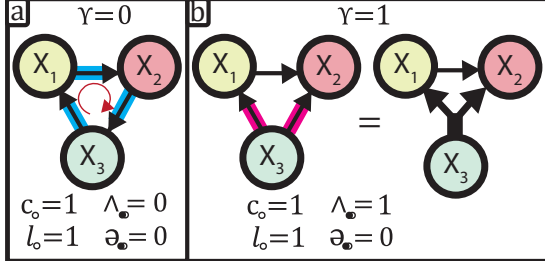
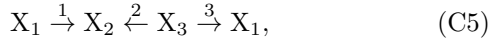
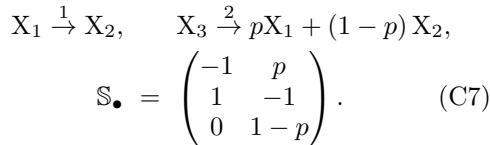


FIG. 10: a) a cyclic CRN composed of irreversible reactions. Cycle reactions are highlighted in blue. Reversing any of the reaction arrows in this cyclic CRN affords CRN b) with co-production index 1. After merging collinear reactions, the original reaction cycle can no longer be performed.



$$\mathbb{S}_\triangleright = \begin{pmatrix} -1 & 0 & 1 \\ 1 & 1 & 0 \\ 0 & -1 & -1 \end{pmatrix}. \quad (\text{C6})$$

For which a cycle (right nullvector) is  $\mathbf{c} = (1, -1, 1)^T$ . We find that  $\Upsilon = 1$ , because  $r_2$  and  $r_3$  are now collinear. Upon merging these we obtain



and by this merger  $\Lambda_\bullet = 1$  cycle is thus lost.

#### Appendix D: Applying laws for isospectral and concealed species

Fig. 11 furnishes further examples of the application of the isospectral species law and the concealed species law.

CRN	$d(X)$	$d(\Lambda)$	$s_\blacksquare$	$b_\square$	$a_\square$	$\S$	$b_\S$	$a_\S$	$r_\sim$
	2	1	0	0	0	1	0	1	0
	2	1	0	0	0	1	0	1	1
	3	2	3	2	1	0	0	0	0
	3	3	2	2	0	0	0	0	0
	2	2	0	0	0	1	1	0	0
	1	1	1	1	0	0	0	0	0
	3	2	2	1	1	0	0	0	0
	3	2	0	0	0	1	0	1	0

FIG. 11: Illustration of laws for isospectral (Eq. (72)) and concealed (Eq. (62)) species for several CRNs. Dark nodes correspond to spectroscopically inactive species. Species that are indistinguishable are marked with a star. New cycles - leading to loss of data dimension - are highlighted in orange and blue. Data dimensions:  $d(X)$ ,  $d(\Lambda)$  (spectral),  $d(X)$  (species).  $d(\Lambda)$  spectral data dimension,  $s_\blacksquare(\Lambda)$ : # concealed species,  $b_\square(\Lambda)$ : # concealed conservation laws,  $a_\square(\Lambda)$ : # apparent cycles,  $\S(\Lambda)$ : isospectral index,  $r_\sim(\Lambda)$ : # isospectral isomerization reactions,  $b_\S(\Lambda)$ : # isospectral broken conservation laws,  $a_\S(\Lambda)$ : #, isospectral emergent cycles.

#### Appendix E: Parametric collinearity

We have considered collinearity that is due to structure alone. For certain combinations of parameters and initial conditions, a CRN may become symmetric and behave like a lower-dimensional CRN. As a concrete example, we consider



For which we previously considered that we have  $r_o = 2$  linearly independent currents

$$J_{1,o} = \kappa_1[A][B] - \kappa_3[C] = J_{1,\triangleright} - J_{3,\triangleright}$$

$$J_{2,o} = \kappa_2[A][B] - \kappa_4[D] = J_{2,\triangleright} - J_{4,\triangleright}$$

and, hence, *a priori*, no collinearity should exist. If we now fix  $[C]_0 = [D]_0$ ,  $\kappa_1 = \kappa_3$ ,  $\kappa_2 = \kappa_4$ , then the rates become collinear  $J_{1,o} = J_{2,o}$  and dynamics for  $[C]$  and  $[D]$  become equivalent, hence we have a conserved quantity:

$$L = [C] - [D] = 0. \quad (\text{E2})$$

This relates to a symmetry in the CRN  $C \leftrightarrow D$ , which vanishes when we let  $[C]_0 \neq [D]_0$ .

This requirement of 3 parametric constraints is readily attained in chemical practice: if C and D are enantiomers in an achiral environment, then the 2 constraints on rate constants will naturally be verified. The constraint  $[C]_0 = [D]_0$  would require that we either add C and D as a racemic mixture, or do not add them at all. We refer to Ref. [114, 115] for

pertinent further decompositions of CRNs with symmetries due to chiral species.

Since parametric collinearity occurs for specific choices of rate constants and initial conditions, it will not generically be detected by algorithmic procedures that seek out conserved quantities.

## ACKNOWLEDGMENTS

A.B. acknowledges support from the EU (Marie-Sklodowska-Curie grant 847675). A.B. acknowledges fruitful discussions with Sijbren Otto. We thank Troy Figiel for drawing our attention to the unexplained conserved quantity in Ref. [76].

- 
- [1] D. V. Kriukov, A. H. Koyuncu, and A. S. Y. Wong, *Small* **18**, 2107523 (2022).
- [2] N. M. Ivanov, M. G. Baltussen, C. L. F. Regueiro, M. T. G. M. Derks, and W. T. S. Huck, *Angew. Chem. Int. Ed.* **62**, e202215759 (2023).
- [3] Y. Zhang, S. Tsitkov, and H. Hess, *Nat Catal* **1**, 276 (2018).
- [4] A. Sharko, B. Spitzbarth, T. M. Hermans, and R. Eelkema, *J. Am. Chem. Soc.* **145**, 9672 (2023).
- [5] N. Singh, G. J. M. Formon, S. De Piccoli, and T. M. Hermans, *Adv. Mater.* **32**, 1906834 (2020).
- [6] S. N. Semenov, A. S. Y. Wong, R. M. van der Made, S. G. J. Postma, J. Groen, H. W. H. van Roekel, T. F. A. de Greef, and W. T. S. Huck, *Nat. Chem.* **7**, 160 (2015).
- [7] L. H. H. Meijer, A. Joesaar, E. Steur, W. Engelen, R. A. van Santen, M. Merckx, and T. F. A. de Greef, *Nat Commun* **8**, 1117 (2017).
- [8] C. Chen, J. S. Valera, T. B. M. Adachi, and T. M. Hermans, *Chem. Eur. J.* **29**, e202202849 (2023).
- [9] M. Ikeda, T. Tanida, T. Yoshii, K. Kurotani, S. Onogi, K. Urayama, and I. Hamachi, *Nat. Chem.* **6**, 511 (2014).
- [10] C. Donau, F. Späth, M. Stasi, A. M. Bergmann, and J. Boekhoven, *Angew. Chem. Int. Ed.* **61**, e202211905 (2022).
- [11] R. Aris, *Arch. Rational Mech. Anal.* **19**, 81 (1965).
- [12] M. Polettni and M. Esposito, *J. Chem. Phys.* **141**, 024117 (2014).
- [13] M. Feinberg, *Foundations of Chemical Reaction Network Theory*, Applied Mathematical Sciences, Vol. 202 (Springer International Publishing, Cham, 2019).
- [14] Y. Sughiyama, A. Kamimura, D. Loutchko, and T. J. Kobayashi, *Phys. Rev. Research* **4**, 033191 (2022).
- [15] S. Dal Cengio, V. Lecomte, and M. Polettni, *Phys. Rev. X* **13**, 021040 (2023).
- [16] F. Avanzini, N. Freitas, and M. Esposito, *Phys. Rev. X* **13**, 021041 (2023).
- [17] J. Schnakenberg, *Rev. Mod. Phys.* **48**, 571 (1976).
- [18] T. L. Hill, *Free Energy Transduction and Biochemical Cycle Kinetics* (Springer New York, New York, NY, 1989).
- [19] J. C. Baez, B. S. Pollard, J. Lorand, and M. Sarazola, Biochemical coupling through emergent conservation laws (2018), arXiv:1806.10764 [q-bio.MN].
- [20] J. C. Baez and B. S. Pollard, *Rev. Math. Phys.* **29**, 1750028 (2017).
- [21] A. Blokhuis, D. Lacoste, and P. Nghe, *Proc. Natl. Acad. Sci. U.S.A.* **117**, 25230 (2020).
- [22] N. Vassena and P. F. Stadler, *Proc. R. Soc. A* **480**, 20230694 (2024).
- [23] A. Deshpande and M. Gopalkrishnan, *Bull Math Biol* **76**, 2570 (2014).
- [24] J. L. Andersen, C. Flamm, D. Merkle, and P. F. Stadler, *Defining Autocatalysis in Chemical Reaction Networks* (2021), arXiv:2107.03086 [cs, q-bio].
- [25] F. Avanzini, M. Bilancioni, V. Cavina, S. D. Cengio, M. Esposito, G. Falasco, D. Forastiere, N. Freitas, A. Garilli, P. E. Harunari, V. Lecomte, A. Lazarescu, S. G. M. Srinivas, C. Moslonka, I. Neri, E. Penocchio, W. D. Piñeros, M. Polettni, A. Raghu, P. Raux, K. Sekimoto, and A. Soret, *SciPost Phys. Lect. Notes*, 80 (2024).
- [26] R. Zhang, Y. Wang, P. Gaspard, and N. Kruse, *Science* **382**, 99 (2023).
- [27] J. P. Unsheber and M. Reiher, *Annu. Rev. Phys. Chem.* **71**, 121 (2020).
- [28] J. S. Manzano, W. Hou, S. S. Zalesskiy, P. Frei, H. Wang, P. J. Kitson, and L. Cronin, *Nat.*



- Chem. **14**, 1311 (2022).
- [29] P. Zhang, N. Weeranoppanant, D. A. Thomas, K. Tahara, T. Stelzer, M. G. Russell, M. O'Mahony, A. S. Myerson, H. Lin, L. P. Kelly, K. F. Jensen, T. F. Jamison, C. Dai, Y. Cui, N. Briggs, R. L. Beingessner, and A. Adamo, *Chem. Eur. J.* **24**, 2776 (2018).
- [30] J. Li, S. G. Ballmer, E. P. Gillis, S. Fujii, M. J. Schmidt, A. M. E. Palazzolo, J. W. Lehmann, G. F. Morehouse, and M. D. Burke, *Science* **347**, 1221 (2015).
- [31] P. J. Kitson, G. Marie, J.-P. Francoia, S. S. Zalesskiy, R. C. Sigerson, J. S. Mathieson, and L. Cronin, *Science* **359**, 314 (2018).
- [32] T. C. Malig, J. D. B. Koenig, H. Situ, N. K. Chehal, P. G. Hultin, and J. E. Hein, *React. Chem. Eng.* **2**, 309 (2017).
- [33] T. C. Malig, Y. Tan, S. R. Wisniewski, C. S. Higman, R. Carrasquillo-Flores, A. Ortiz, G. E. Purdum, S. Kolotuchin, and J. E. Hein, *React. Chem. Eng.* **5**, 1421 (2020).
- [34] C. Rougeot, H. Situ, B. H. Cao, V. Vlachos, and J. E. Hein, *React. Chem. Eng.* **2**, 226 (2017).
- [35] U. Bentrup, *Chem. Soc. Rev.* **39**, 4718 (2010).
- [36] R. Theron, Y. Wu, L. P. E. Yunker, A. V. Hesketh, I. Pernik, A. S. Weller, and J. S. McIndoe, *ACS Catal.* **6**, 6911 (2016).
- [37] L. Jašíková, M. Anania, S. Hybelbauerová, and J. Roithová, *J. Am. Chem. Soc.* **137**, 13647 (2015).
- [38] R. Hilgers, S. Yong Teng, A. Briš, A. Y. Pereverzev, P. White, J. J. Jansen, and J. Roithová, *Angew. Chem. Int. Ed.* **61**, e202205720 (2022).
- [39] Y. Geiger, T. Achard, A. Maise-François, and S. Bellemin-Lapponnaz, *Nat Catal* **3**, 422 (2020).
- [40] D. G. Blackmond, *Acc. Chem. Res.* **33**, 402 (2000).
- [41] C. Puchot, O. Samuel, E. Dunach, S. Zhao, C. Agami, and H. B. Kagan, *J. Am. Chem. Soc.* **108**, 2353 (1986).
- [42] R. Pollice and M. Schnürch, *Chem. Eur. J.* **22**, 5637 (2016).
- [43] R. Chouket, A. Pellissier-Tanon, A. Lahlou, R. Zhang, D. Kim, M.-A. Plamont, M. Zhang, X. Zhang, P. Xu, N. Desprat, D. Bourgeois, A. Espagne, A. Lemarchand, T. L. Saux, and L. Jullien, *Nat Commun* **13**, 1482 (2022).
- [44] F. Closa, C. Gosse, L. Jullien, and A. Lemarchand, *J. Chem. Phys.* **142**, 174108 (2015).
- [45] D. G. Blackmond, *J. Am. Chem. Soc.* **137**, 10852 (2015).
- [46] A. J. Kałka and A. M. Turek, *J Fluoresc* **31**, 1599 (2021).
- [47] M. Garrido, F. X. Rius, and M. S. Larrechi, *Anal. Bioanal. Chem.* **390**, 2059 (2008).
- [48] S. D. Frans and J. M. Harris, *Anal. Chem.* **56**, 466 (1984).
- [49] C. Ruckebusch, B. Walczak, and L. Buydens, eds., *Resolving spectral mixtures: with applications from ultrafast time-resolved spectroscopy to super-resolution imaging*, first edition ed., Data handling in science and technology No. volume 30 (Elsevier, Amsterdam ; Boston, 2016) oCLC: ocn950449764.
- [50] S. Bijlsma, H. F. M. Boelens, and A. K. Smilde, *Appl Spectrosc* **55**, 77 (2001).
- [51] A. Voronov, A. Urakawa, W. v. Beek, N. E. Tsakoumis, H. Emerich, and M. Rønning, *Anal. Chim. Acta* **840**, 20 (2014).
- [52] Y. B. Monakhova, S. A. Astakhov, A. Kraskov, and S. P. Mushtakova, *Chemom. Intell. Lab. Syst.* **103**, 108 (2010).
- [53] Y. B. Monakhova, S. P. Mushtakova, S. S. Kolesnikova, and S. A. Astakhov, *Anal. Bioanal. Chem.* **397**, 1297 (2010).
- [54] A. D. Vogt and E. Di Cera, *Biochemistry* **51**, 5894 (2012).
- [55] S. Gianni, J. Dogan, and P. Jemth, *Biophys. Chem.* **189**, 33 (2014).
- [56] T. Morton, D. Mysza, and I. Chaiken, *Analytical Biochemistry* **227**, 176 (1995).
- [57] M. G. Baltussen, J. van de Wiel, C. L. Fernández Regueiro, M. Jakštaitė, and W. T. S. Huck, *Anal. Chem.* **94**, 7311 (2022).
- [58] X. Li and A. B. Kolomeisky, *J. Chem. Phys.* **139**, 144106 (2013).
- [59] A. L. Thorneywork, J. Gladrow, Y. Qing, M. Rico-Pasto, F. Ritort, H. Bayley, A. B. Kolomeisky, and U. F. Keyser, *Sci. Adv.* **6**, eaaz4642 (2020).
- [60] D. G. Blackmond, *Angew. Chem. Int. Ed.* **44**, 4302 (2005).
- [61] J. Burés, *Angew. Chem. Int. Ed.* **55**, 2028 (2016).
- [62] J. Burés, *Angew. Chem. Int. Ed.* **55**, 16084 (2016).
- [63] R. Pollice, *ChemRxiv* 10.26434/chemrxiv.7885760.v1 (2019).
- [64] R. Aris and R. H. S. Mah, *Ind. Eng. Chem. Fund.* **2**, 90 (1963).
- [65] M. Feinberg, *Arch. Rational Mech. Anal.* **49**, 187 (1972).
- [66] F. Horn, *Arch. Rational Mech. Anal.* **49**, 172 (1972).
- [67] Y. Hirono, T. Okada, H. Miyazaki, and Y. Hidaka, *Phys. Rev. Research* **3**, 043123 (2021).
- [68] D. Kondepudi and I. Prigogine, *Modern Thermodynamics: From Heat Engines to Dissipative Structures*, 1st ed. (Wiley, 2014).
- [69] T. Aslyamov, F. Avanzini, E. Fodor, and M. Esposito, *Phys. Rev. Lett.* **131**, 138301 (2023).
- [70] E. Penocchio, R. Rao, and M. Esposito, *J. Chem. Phys.* **155**, 114101 (2021).
- [71] A. Blokhuis, D. Lacoste, and P. Gaspard, *J. Chem. Phys.* **148**, 144902 (2018).
- [72] J. M. Poulton, P. R. ten Wolde, and T. E. Ouldridge, *Proc. Natl. Acad. Sci. U.S.A.* **116**, 1946 (2019).
- [73] P. Gaspard and R. Kapral, *J. Chem. Phys.* **148**, 134104 (2018).
- [74] M. Poletini, A. Wachtel, and M. Esposito, *J. Chem. Phys.* **143**, 184103 (2015).
- [75] L. Oberreiter, U. Seifert, and A. C. Barato, *Phys. Rev. E* **106**, 014106 (2022).

- [76] Z. Liu, P. O. Sturm, S. Bharadwaj, S. J. Silva, and M. Tegmark, *Phys. Rev. E* **109**, L023301 (2024).
- [77] S. E. Braslavsky, *Pure Appl. Chem.* **79**, 293 (2007).
- [78] F. Kaspar, *ChemBioChem* **24**, e202200744 (2023).
- [79] M. D. Cohen and E. Fischer, *J. Chem. Soc.*, 3044 (1962).
- [80] G. Scheibe, *Angew. Chem.* **50**, 212 (1937).
- [81] Although no mention is made of conserved quantities, Cohen and Fischer have reported on this phenomenon in their work on conditions for the occurrence of isosbestic points[79], by arguing that while  $B \leftarrow A \rightarrow C$  has 2 reactions, their simultaneity still enables an isosbestic point.
- [82] Another scenario where irreversible reactions can be used is for reactions with driving forces fixed (e.g. phase reactions, reactions with chemostatted concentrations) in such a way that their rates remain fixed. A reversible and irreversible description of the reaction would yield the same fixed rate (but only one the former can be linked to thermodynamics).
- [83] K. I. Öberg, *Chem. Rev.* **116**, 9631 (2016).
- [84] Millar, T. J., Walsh, C., Van de Sande, M., and Markwick, A. J., *Astron. Astrophys.* **682**, A109 (2024).
- [85] N. Indriolo and B. J. McCall, *Chem. Soc. Rev.* **42**, 7763 (2013).
- [86] G. B. Boursalian, E. R. Nijboer, R. Dorel, L. Pfeifer, O. Markovitch, A. Blokhuis, and B. L. Feringa, *J. Am. Chem. Soc.* **142**, 16868 (2020).
- [87] V. García-López, D. Liu, and J. M. Tour, *Chem. Rev.* **120**, 79 (2020).
- [88] R. A. Cox, *Chem. Rev.* **103**, 4533 (2003).
- [89] P. O. Sturm and A. S. Wexler, *Geosci. Model Dev.* **15**, 3417 (2022).
- [90] H. Herrmann, T. Schaefer, A. Tilgner, S. A. Styler, C. Weller, M. Teich, and T. Otto, *Chem. Rev.* **115**, 4259 (2015).
- [91] There exist further decompositions of  $\ell_o$  for open systems. For instance, mass-like conservation laws with purely positive entries are used to describe moiety conservation in biochemistry[116, 117]. Charge-like conservation laws - with coefficients of mixed sign - can always be eliminated in a closed system[118], in favor of a basis with purely positive conservation laws[119, 120]. This is not true for an open system, e.g.  $A + B \rightleftharpoons \emptyset$  has as its  $\ell_o = 1$  unique conservation law the charge-like quantity  $[A] - [B] = L$ .
- [92] Some authors investigate CRNs with current functions that are not mass-action[13, 22], allowing to generalize results to larger classes of dynamical systems. E.g. N. Vassena defines current functions as *chemical* when they are nonnegative and monotonically increasing functions depending only on reactant concentration(s). Co-production can occur for more general classes of current functions, but need then no longer be implied by reactant stoichiometry.
- [93] Note that in a stochastic description where deterministic  $[A]$ ,  $[B]$  are replaced with fluctuating  $n_A$ ,  $n_B$ , the collinear reactions still occur independently. Hence, the stochastic analogue of the conserved quantity is not conserved intrinsically,  $\kappa_2 n_A - \kappa_1 n_B \neq 0$ . Instead it holds on average,  $\kappa_2 \langle n_A \rangle - \kappa_1 \langle n_B \rangle = 0$ , and thus imposes a constraint on statistical momenta.
- [94] There are other sources of emergent conserved quantities that SID may detect. For instance, Hirono et al have listed 3 types of systems exhibiting emergent conserved quantities[67] characterized as 'pathological': CRNs i) requiring extra parameters to specify steady-state, ii) having no steady-state, iii) having unphysical kinetics. Bazhin and Baez et al have discussed conservation laws underlying biochemical coupling[19, 121], which are conservation laws that are valid for a subnetwork of fast reactions (and hence respected on short time approximations of the time evolution of species abundances).
- [95] H. Barrington, A. Dickinson, J. McGuire, C. Yan, and M. Reid, *Org. Process Res. Dev.* **26**, 3073 (2022).
- [96] C. Yan, M. Cowie, C. Howcutt, K. M. P. Wheelhouse, N. S. Hodnett, M. Kollie, M. Gildea, M. H. Goodfellow, and M. Reid, *Chem. Sci.* **14**, 5323 (2023).
- [97] J. Daglish, A. J. Blacker, G. de Boer, A. Crampton, D. R. J. Hose, A. R. Parsons, and N. Kapur, *Org. Process Res. Dev.* **27**, 627 (2023).
- [98] V. A. Marčenko and L. A. Pastur, *Math. USSR Sb.* **1**, 457 (1967).
- [99] D. Venturi, *J. Fluid Mech.* **559**, 215 (2006).
- [100] B. P. Epps and E. M. Krivitzky, *Exp Fluids* **60**, 121 (2019).
- [101] B. P. Epps and A. H. Techet, *Exp Fluids* **48**, 355 (2010).
- [102] S. Batzner, A. Musaelian, L. Sun, M. Geiger, J. P. Mailoa, M. Kornbluth, N. Molinari, T. E. Smidt, and B. Kozinsky, *Nat Commun* **13**, 2453 (2022).
- [103] S. L. Brunton, J. L. Proctor, and J. N. Kutz, *Proc. Natl. Acad. Sci. U.S.A.* **113**, 3932 (2016).
- [104] M. Schmidt and H. Lipson, *Science* **324**, 81 (2009).
- [105] Y.-i. Mototake, *Phys. Rev. E* **103**, 033303 (2021).
- [106] S. J. Wetzel, R. G. Melko, J. Scott, M. Panju, and V. Ganesh, *Phys. Rev. Res.* **2**, 033499 (2020).
- [107] C. J. Taylor, H. Seki, F. M. Dannheim, M. J. Willis, G. Clemens, B. A. Taylor, T. W. Chamberlain, and R. A. Bourne, *React. Chem. Eng.* **6**, 1404 (2021).
- [108] M. J. Willis and M. v. Stosch, *Comput. Chem. Eng.* **90**, 31 (2016).
- [109] J. Burés and I. Larrosa, *Nature* **613**, 689 (2023).

- [110] W. Ji and S. Deng, J. Phys. Chem. A **125**, 1082 (2021).
- [111] M. Polettini and M. Esposito, Phys. Rev. Lett. **119**, 240601 (2017).
- [112]  $CQ_3$  was taken from the Supp. Matt. of Ref[76] where it is derived. It differs from the expression for  $CQ_3$  due to a small typo for the coefficient of  $[OH^\bullet]$ .
- [113] As SID is a numerical algorithm, this is done in practice by checking  $P$  randomly chosen points. As long as the phase space functions and the flow equations are polynomial, as is the case here, sufficiently large  $P$  will ensure that  $H(x)$  is conserved for all  $x$ .
- [114] G. Laurent, D. Lacoste, and P. Gaspard, Proc. Natl. Acad. Sci. U.S.A. **118**, e2012741118 (2021).
- [115] G. Laurent, P. Gaspard, and D. Lacoste, Proc. R. Soc. A **478**, 20210590 (2022).
- [116] J.-H. S. Hofmeyr, H. Kacser, and K. J. Merwe, Eur. J. Biochem. **155**, 631 (1986).
- [117] F. Avanzini and M. Esposito, J. Chem. Phys. **156**, 014116 (2022).
- [118] A. Blokhuis, *Physical aspects of origins of life scenarios*, Thesis, Université Paris sciences et lettres (2019).
- [119] S. Schuster and T. Höfer, Faraday Trans. **87**, 2561 (1991).
- [120] S. Müller, C. Flamm, and P. F. Stader, J. Cheminform. **14**, 63 (2022).
- [121] N. Bazhin, ISRN Biochem. **2012**, 1 (2012).